

The control of charge and spin density localization in a double quantum dot at the edge of the topological insulator as the physical background of the qubit operations

© E.A. Lavrukhina¹, D.V. Khomitsky²

¹ Physical and Technical Research Institute, National Research State University of Nizhny Novgorod, 603022 Nizhny Novgorod, Russia

² Department of Physics, National Research State University of Nizhny Novgorod, 603022 Nizhny Novgorod, Russia

E-mail: ekaterina.a.lavrukhina@gmail.com

Received June 23, 2025

Revised August 14, 2025

Accepted August 14, 2025

The methods of control of the spatial localization and spin polarization are studied for the model of double quantum dot at the edge of topological insulator based on HgTe/CdTe quantum well and formed by three magnetic barriers. The transitions in the spectrum induced by the resonance electric field are found for which the initial and final states correspond to the different spatial localization or to the specific sign of the chosen spin projection. Based on these transitions, the possibility of the information encoding is demonstrated for modeling of the coupled charged and spin qubits and for some of the qubit operations including the single-qubit NOT, Z and two-qubit CNOT.

Keywords: topological insulator, magnetic barrier, double quantum dot, localization, charge qubit, spin qubit.

DOI: 10.61011/SC.2025.06.62057.7732

1. Introduction

Topological insulators (TI), in particular two-dimensional TI based on HgTe/Cd_xHg_{1-x}Te quantum wells [1,2] have been experimentally and theoretically studied for about 20 years. Many fundamental and applied results have been obtained during this period, but progress in their technological and instrumental applications is more modest. This is partly due to the unique properties of the edge states in TI, which are stable from scattering by non-magnetic impurities and propagate over significant distances, on the order of several microns, along the edge of the sample [2]. At the same time, it turns out to be much more difficult to construct compact objects of the form of quantum dots (QDs) for subsequent use, in particular in quantum computing problems [3]. This is attributable to the difficulties in creating localized functions from edge states in a purely electric field, while a magnetic field destroys topological security. Nevertheless, theoretical models of quantum dots with magnetic barriers have been known for many years [4–6]. In our previous work, we developed the models of single [7–9] and double [10] QD with magnetic barriers of finite permeability based on dielectric magnets. It was shown that there are a variable number of discrete levels depending on the height and orientation of the magnetization of the barriers [9], as well as the presence of continuous spectrum states above the barriers. The possibilities of controlling the populations of discrete levels in a periodic electric field were studied in Ref. [8].

In this paper, we continue to study the model of a double quantum dot on the TI edge based on the

HgTe/Cd_xHg_{1-x}Te quantum well formed by three magnetic barriers, which was started in Ref. [10]. The main emphasis is placed on the control of spatial localization and the associated spin polarization of states depending on the orientation of the magnetization of the barriers. It is shown that a change in the orientation of only one central barrier can affect localization and spin polarization over a wide range. Based on the predicted properties, we propose encoding schemes for the states of two qubits in the system under consideration. The first qubit can be called a charge qubit, and spatial localization of the wave function is used for encoding. The second qubit can be called a spin qubit, and the spin projection is used for encoding. The possibilities of organizing basic quantum computing operations in such a qubit system, such as the NOT and Z gates, as well as the two-qubit CNOT operation, are discussed when the system is exposed to a resonant electric field.

We limit ourselves to solving the problem within the framework of the single-particle Schrodinger equation, without including relaxation effects. Some estimates of such effects were obtained earlier by us [7], others are given in this paper. They say that at sufficiently low temperatures, which are common for qubit systems (1 K and lower), it is possible to perform the operations under discussion. In addition, our model allows you to switch between system states (gates), as transitions between its various stationary states for fixed system parameters. The results obtained allow us to hope for the application of structures with a double quantum dot at the edge of the TI, including in quantum computing tasks.

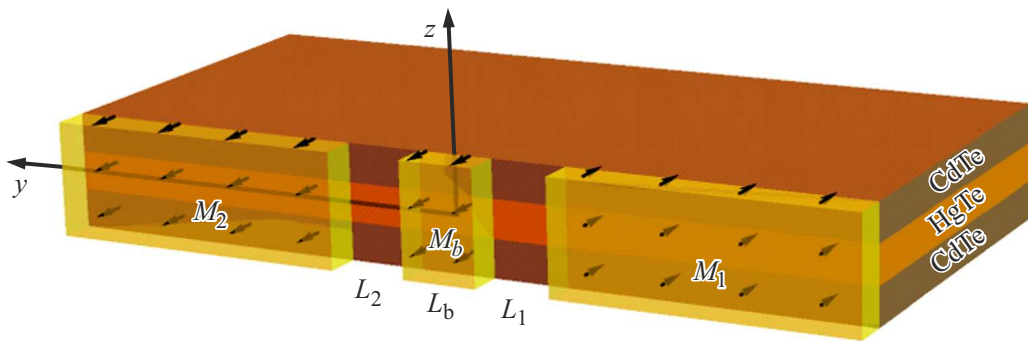


Figure 1. A model of a double quantum dot formed on the one-dimensional TI edge by magnetic barriers, described by the Hamiltonian (1). L_1, L_2 — widths of quantum dots, L_b — width of the central barrier, M_1, M_b, M_2 — barrier heights in energy units.

2. Model and properties of states

We use the model of double QD on the edge of TI with $\text{HgTe}/\text{Cd}_x\text{Hg}_{1-x}\text{Te}$ quantum well, developed by us in Ref. [10]. In this model, we consider a sequence of three magnetic barriers located at the TI edge, between which two regions of quantum dots are formed, as shown in Figure 1. The Hamiltonian of the system has the form

$$\begin{aligned} H = & A k_y \sigma_z - M_1 S(-L_1 - y) (\sigma_x \cos \theta_1 + \sigma_y \sin \theta_1) \\ & - M_b (S(y) - S(y - L_b)) (\sigma_x \cos \theta_b + \sigma_y \sin \theta_b) \\ & - M_2 S(y - L_b - L_2) (\sigma_x \cos \theta_2 + \sigma_y \sin \theta_2). \end{aligned} \quad (1)$$

In (1), the first term $A k_y \sigma_z$ corresponds to the kinetic energy of one-dimensional edge states in TI [1], where the parameter $A = 360 \text{ meV} \cdot \text{nm}$. The remaining terms describe the energy of interaction with three magnetic barriers located in regions $y < -L_1$, $0 < y < L_b$ and $y > L_b + L_2$, respectively, and having a profile described by the step function $S(y)$, as shown in Figure 1. The amplitudes of interaction with barriers in energy units are M_1, M_b, M_2 , angles $\theta_1, \theta_b, \theta_2$ set the orientation the magnetization of the barriers in the plane (xy) , where $\theta = 0$ corresponds to the orientation along the axis Ox in Figure 1. Boundary conditions, wave functions, and the energy spectrum of the Hamiltonian (1) discussed in Ref. [10]. It was also shown that with mutually opposite orientations of the magnetization of the extreme barriers $\theta_1 = 0, \theta_2 = \pi$, depending on the orientation of the magnetization of the central barrier, localization of the wave function occurs, as shown in Figure 2, *a* for the ratio P of the contributions of states in the left and right QD. Here, the orange color means localization in the left QD at $P \gg 1$, and blue — in right QD at $P \ll 1$. The scale in Figure 2, *a* does not allow showing the small gaps that form at the intersection points of the levels at $\theta_b = \pi/2, 3\pi/2$, i.e., there is anti-crossing in the spectrum [10].

The question arises about the effect on the electronic spectrum shown in Figure 2, *a* and *b* of the Coulomb

interaction between particles corresponding to filled states below the Fermi level when the polarization of the central barrier changes. To estimate the energy order of the E_C Coulomb interaction, we use the expression

$$E_C \sim e^2/(\epsilon L). \quad (2)$$

In (2) $L \sim L_1 \sim L_2 \sim 100 \text{ nm}$ is the distance between the maxima of the wave function in the spectrum for states closest to each other in the spectrum and located below the Fermi level, which are shown in Figure 2, *a*. In terms of the order of magnitude, L corresponds to the size of the quantum dot $L_1(L_2)$ [10]. The constant $\epsilon \sim 20$ is the low-frequency permittivity of the bulk HgTe [11], which can decrease by 10–20 % in the HgTe quantum well depending on the electron concentration [12]. We obtain $E_C \sim 1 \text{ meV}$ after substituting the specified parameters in (2). The characteristic kinetic energy of the electrons in the spectrum in Figure 2 is comparable to the energy of discrete states and is of the order of $E_n \sim 5–15 \text{ meV}$ for most of the levels used in our calculations. This means that the condition $E_C/E_n \sim 0.05–0.2$ is fulfilled for the main fraction of states, which allows, to a first approximation, not to take into account the Coulomb interaction with states located below the Fermi level. For subsequent approximations, this account will already be required, which, however, is beyond the scope of this work.

3. Encoding information and operations with qubits in charge and spin subsystems

The behavior of the function P , which describes the localization of the wave function in Figure 2, *a*, suggests the possibility of using states with certain localization regions in left and right QD with a fixed orientation of the magnetization θ_b of the central barrier as the basis of the „charge“ qubit for encoding information. As an example, in Figure 2, *a*, the points *a*, *b*, *c*, *d* are marked, of which the points *a* and *c* correspond to the localization of states in the

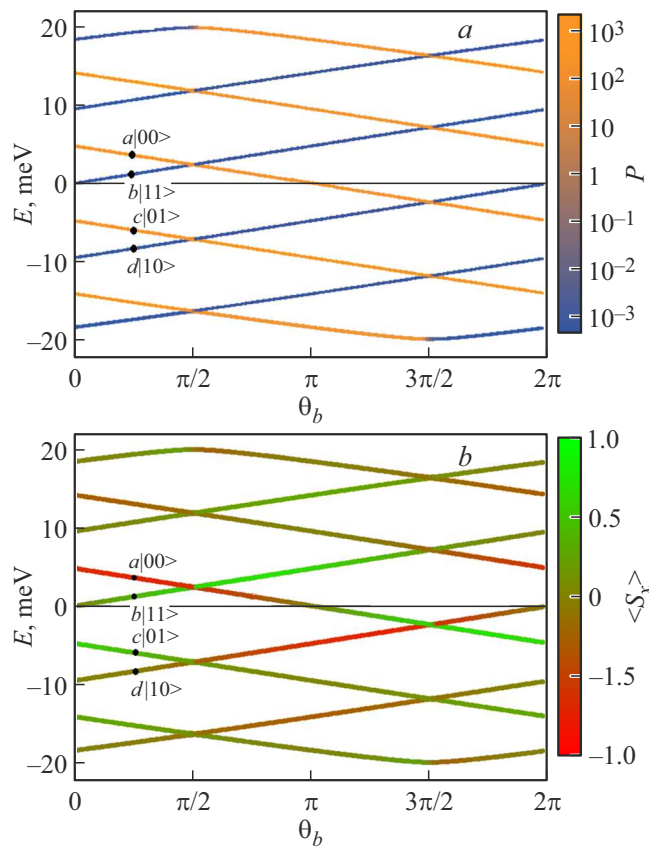


Figure 2. *a* — localization function P depending on the energy E and the magnetization angle of the central barrier θ_b for parameters in (1) $\theta_1 = 0$, $\theta_2 = \pi$, L_1 , L_2 and $L_b = 100$ nm, M_1 , M_2 and $M_b = 20$ meV. The blue color corresponds to localization in the right QD scan at $P \ll 1$, orange — localization in left QD at $P \gg 1$; *b* — dependence of the average value of the spin projection $\langle S_x \rangle$ on E and θ_b at the same parameters. For (a) and (b) pairs of points *a* and *b* (or *c* and *d*) for a fixed θ_b , the answers are different localization and different sign $\langle S_x \rangle$. The encoding of the states of the system (3) of two coupled charge and spin qubits is indicated next to the points.

left QD, and points *b* and *d* correspond to the localization of states in the right QD. Their spatial localization allows talking about the possibility of encoding states of the form $|0\rangle$ and $|1\rangle$ for a charge or spatial qubit, where the state $|0\rangle$ is attributed to the values $P \gg 1$, i.e. on the orange branch of the spectrum, and the state of $|1\rangle$ is attributed to the values of $P \ll 1$, i.e., the blue branch of the spectrum. With this approach, the points *a* and *c* in Figure 2, *a* correspond to the same, i.e., the first state $|0\rangle$ of the charge qubit, and the points *b* and *d* correspond to its second state $|1\rangle$. The transition between these states is possible, for example, when an electric field pulse is applied at the resonant frequency $\omega_{ac} = E_a - E_c$ or $\omega_{bd} = E_b - E_d$ [8], depending on which QD the electron is localized in. It should be noted that even if the frequencies ω_{ac} and ω_{bd} exactly match, transitions between these pairs of levels can be induced independently, since the wave functions of the

initial and final states in each pair are localized at different quantum dots. Accordingly, the localization of the electric field causing the transitions in the region of a specific QD will cause transitions between only one pair of levels.

The question arises — what are the properties of the spin projections of the Hamiltonian states (1) and is it also possible to use them to encode information. It is known that the average value of the z -projection of spin of a two-component spinor, which is an eigenfunction of the Hamiltonian (1), is zero [9]. The other two projections depend significantly on the energy and, as we will see, on the spatial localization of the wave function. Figure 2, *b* shows a graph of the distribution of the average value of x -projections of spin $\langle S_x \rangle$ (in units $\hbar/2$) for the same energy levels and the same parameters that answers Figure 2, *a*. From the comparison of Figure 2, *a* and *b*, it can be concluded that the sign of $\langle S_x \rangle$ can change in case of the change of the spatial localization area of the wave function, which corresponds to the transition between the orange and blue branches in Figure 2, *a*. By analogy with encoding information through spatial localization, we can repeat the reasoning for encoding the states of the second, „spin“ qubit in our system using the sign of the spin projection, for example, $\langle S_x \rangle$, the graph for which is shown in Figure 2, *b*. The state $|0\rangle$ of this qubit can be attributed to the negative values of the projection $\langle S_x \rangle$, shown in shades of orange in Figure 2, *b*. The state $|1\rangle$ of the spin qubit, respectively, will correspond to the positive sign of the projection $\langle S_x \rangle$, shown in shades of green in Figure 2, *b*. Then the state $|0\rangle$ will correspond to points *a* and *d* in Figure 2, *b* with the same projection sign $\langle S_x \rangle$, and the state $|1\rangle$ of the spin qubit will correspond to points *b* and *c*, respectively.

The discussions conducted for the spatial localization in Figure 2, *a* and for the spin projection $\langle S_x \rangle$ in Figure 2, *b* allow speaking about the description of two related subsystems, charge and spin, which can be referred as a charge qubit and a spin qubit. The following states of a two-qubit system can be assigned using this language to the points *a*, *b*, *c*, *d* in Figure 2, *a* and *b*, where the first position corresponds to the charge qubit, and the second position corresponds to the spin qubit:

$$a \rightarrow |00\rangle; b \rightarrow |11\rangle; c \rightarrow |01\rangle; d \rightarrow |10\rangle. \quad (3)$$

First, we will discuss possible schemes for implementing some single-qubit operations, taking into account encoding (3), and then the two-qubit operation CNOT. These operations can be performed by applying control pulses of an electric field that cause transitions between the states of the discrete spectrum in the QDs under consideration, as discussed in Ref. [10]. In this paper, we will discuss only a qualitative schematic diagram of such transitions.

3.1. Single-qubit operation NOT, charge qubit

This operation can be implemented with a resonant transition between the levels *a* and *b* or *c* and *d* in Figure 2,

depending on the position of the Fermi level. The final state must be free to ensure upward energy transitions, which can be achieved by appropriately shifting the Fermi level when the potentials of the control electrodes change.

3.2. Single-qubit operation NOT, spin qubit

This operation can be implemented similarly to the previous one, only transitions must be performed at a resonant frequency between pairs of levels a and c or b and d in Figure 2. It should be noted that this time the difference between the pairs of levels between which transitions take place, in addition to the energy of the levels, also consists in the different spatial localization of the wave functions, which is explained by the different color of the lines in Figure 2, a .

3.3. Single-qubit operations Z, charge and spin qubits

The one-qubit operation Z consists of multiplying the state vector from the left by the Pauli matrix σ_z , converting the state $\alpha|a\rangle + \beta|b\rangle$ to the state $\alpha|a\rangle - \beta|b\rangle$. It is known that it can be implemented for a two-tier system, i.e. for both the charge and spin qubits, simply in the course of the free evolution of the state [3]. Let us consider, for example, the evolution of a linear combination of states $|a\rangle$ and $|c\rangle$ forming the basis of a spin qubit in Figure 2, i.e., a function of the form $\psi(t=0) = \alpha|a\rangle + \beta|c\rangle$, where α and β are arbitrary constants. Indeed, the energies of the states, for example, at points a and c in Figure 2, a and b differ in sign, i.e., $E_a = E_0$ and $E_c = -E_0$. If we select a time point from the start of the countdown at $t_n = (\pi + 4\pi n)\hbar/2E_0$, where $n = 0, 1, 2, \dots$, then after taking out the total phase multiplier, we get a combination in which the contribution of the state $|c\rangle$ will differ by the phase π from the contribution of the state a , i.e., we will have $\psi(t=t_n) = \alpha|a\rangle - \beta|c\rangle$, which is the implementation of the operation Z . Similar arguments can be carried out for a linear combination of states a, d or b, c corresponding to the basis of the charge qubit.

3.4. Two-qubit CNOT operation

As you know, the CNOT operation leaves a pair of two-qubit states $|00\rangle$ and $|01\rangle$ unchanged, and the states $|10\rangle$ and $|11\rangle$ swap [3]. In encoding (3), this means that there should be no transition between the points a and c in Figure 2, a and b , but the transition is implemented between the points b and d . These pairs of points correspond, according to Figure 2, a , to different spatial localization of the wave function in left or in right QD, respectively. It can be assumed that this transition can be implemented under the condition that a control action, for example, an alternating electric field, causing transitions between states with different spin projections $\langle S_x \rangle$ at a resonant frequency $\omega_{bd} = E_b - E_d$, is localized in the region

of only the right QD, to which the pair the points b and d correspond. This can be achieved by an appropriate configuration of the control gates. In this case, when the charge qubit is in the state $|0\rangle$ with the localization of the wave function in the left QD, the transition between the points a and c will not take place, since the field will not affect the wave function. On the contrary, when the charge qubit is in the state $|1\rangle$ with the localization of the wave function in the right QD will transition between the points b and d , i.e. between the states $|0\rangle$ and $|1\rangle$ of the spin qubit. As a result, we will get the implementation of the CNOT operation.

3.5. The switching speed of a spin qubit in an external electric field

In conclusion, we will estimate the speed of the CNOT operation for a spin qubit in a periodic electric field with frequency, when a transition occurs between the states a and c or b and d in Figure 2. Similar estimates can be obtained for charge qubit operations. In the dipole approximation for the geometry of our structure in Figure 1 the matrix element of the transition is the matrix element of the coordinate operator y [8]. It should be noted that a nonzero amplitude $|y_{mn}|$ for transitions between states with close to opposite spin projection can occur for the Hamiltonian (1). It is the first term in (1) that has the form of a contribution from the strong spin-orbit interaction. It is known that the combined spinor wave function for spin 1/2 has the form $(\psi_1(r), \psi_2(r))$ in the presence of SOB, where components 1 and 2, generally speaking, are not reduced to one spatial multiplier $\psi(r)$. In this case, the matrix element y_{mn} may have a nonzero value even for states with close to antiparallel spin orientation. This is the basis for the widely used method of electric dipole spin resonance for manipulating spin in semiconductor structures with strong SOB using an electric field. An example of

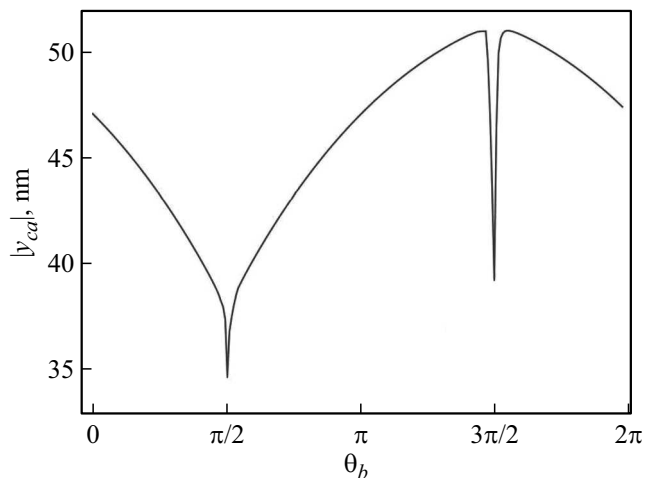


Figure 3. Dependence of the module $|y_{ca}|$ of the dipole matrix element for a pair of states c and a in Figures 1 and 2 as a function of the magnetization angle of the barrier θ_b .

the dependence of $|y_{mn}|$ on θ_b , obtained by numerical calculation for the states of the Hamiltonian (1) described in Ref. [10], is shown in Figure 3, for a pair of states c and a in Figures 1 and 2, characterized by the opposite sign of the projection $\langle S_x \rangle$. It can be concluded from Figure 3 that for the considered pair of states, the value of $|y_{ca}|$ is up to 40–50 nm, depending on the barrier angle θ_b . For such a dipole matrix element, the characteristic value of the Rabi frequency $\Omega = F|y_{mn}|/\hbar$ for qubit switching in an electric field with a voltage of $F \sim 0.03\text{--}0.09 \text{ meV/nm}$ reaches values of $(2\text{--}10) \cdot 10^{12} \text{ s}^{-1}$. This estimate suggests that the spin qubit in our system is capable of operating in the terahertz mode, which is very promising for applications in quantum computing. Detailed calculations of the dynamics of transitions, including taking into account relaxation and decoherence, may be an interesting task for future studies.

4. Conclusion

A model is constructed and the properties of localization of states and their spin projections are studied for a double quantum dot at the edge of a topological insulator formed by three magnetic barriers. It is shown that different states of the discrete spectrum correspond to both different regions of the spatial localization of the electron in left or right quantum dots, and different selected spin projections. The possibility of encoding information for two subsystems, charge and spin, corresponding to the implementation of spatial and spin qubits is proposed on this basis. Schemes of some single-qubit and one two-qubit operations are also considered, which can be represented in the specified encoding if transitions between states of a discrete spectrum in a resonant electric field are carried out. The dynamics of these transitions, together with the calculation of errors and the calculation of reliability (fidelity) of operations, as well as the construction of diagrams of other gates (Hadamard and others) within the framework of the proposed model, may be a topic for future work.

Funding

The work was supported by the Ministry of Science and Higher Education of the RF under State Assignment FSWR-2023-0035.

Acknowledgments

The authors would like to express their gratitude to D.S. Pashin, M.V. Bastrakova, and Z.F. Krasilnik, V.Ya. Alyoshkin, V.I. Gavrilenko and many other participants of 29th Symposium „Nanophysics and Nanoelectronics“ for a number of useful comments.

Conflict of interest

The authors declare no conflict of interest.

References

- [1] X.-L. Qi, S.-C. Zhang. *Rev. Mod. Phys.*, **83**, 1057 (2011). DOI: 10.1103/RevModPhys.83.1057
- [2] Z.D. Kvon, D.A. Kozlov, E.B. Olshanetsky, G.M. Gusev, N.N. Mikhailov, S.A. Dvoretsky. *UFN*, **190** (7), 673 (2020). (in Russian). DOI: 10.3367/UFNr.2019.10.038669
- [3] M.A. Nielsen, I.L. Chuang. *Quantum Computation and Quantum Information*, 10th Anniversary edn (N.Y., Cambridge University Press, 2010) Chap. 1.3. DOI: 10.1017/CBO9780511976667
- [4] C. Timm. *Phys. Rev. B*, **86**, 155456 (2012). DOI: 10.1103/PhysRevB.86.155456
- [5] G. Dolcetto, N. Traverso Ziani, M. Biggio, F. Cavalieri, M. Sassetti. *Phys. Rev. B*, **87**, 235423 (2013). DOI: 10.1103/PhysRevB.87.235423
- [6] G.J. Ferreira, D. Loss. *Phys. Rev. Lett.*, **111**, 106802 (2013). DOI: 10.1103/PhysRevLett.111.106802
- [7] D.V. Khomitsky, E.A. Lavrukhina, A.A. Chubanov, N. Nzhiiya. *FTP*, **51** (11), 1557 (2017). (in Russian). DOI: 10.21883/FTP.2017.11.45111.25
- [8] D.V. Khomitsky, K.S. Kabaev, E.A. Lavrukhina. *ZhETF*, **158** (5), 929 (2020). (in Russian). DOI: 10.31857/S0044451020110152
- [9] D.V. Khomitsky, A.A. Konakov, E.A. Lavrukhina. *J. Phys.: Condens. Matter*, **34**, 405302 (2022). DOI: 10.1088/1361-648X/ac8407
- [10] E.A. Lavrukhina, D.V. Khomitsky, A.V. Doleznikov. *FTP*, **57** (7), 551 (2023). (in Russian). DOI: 10.61011/FTP.2023.07.56788.4943C
- [11] A. Rogalski. *Rep. Progr. Phys.*, **68**, 2267 (2005). DOI: 10.1088/0034-4885/68/10/R01
- [12] V.Ya. Aleshkin, A.V. Germanenko, G.M. Miknov, A.A. Shershtobitov. *Physica E*, **128**, 114606 (2021). DOI: 10.1016/j.physe.2020.114606

Translated by A.Akhtyamov